*Chapter 6*

# FREQUENCY STABILITY

## 6.1 Frequency Stability of a Passive Atomic Frequency Standard

This section calculates the frequency stability of a passive atomic frequency standard, which depends on the width of the atomic resonance signal, the sensitivity of the atomic resonance measurement, the free-running phase noise and the bandwidth of the frequency control loop. Many atomic clocks use a simple integrator to lock the voltage-controlled oscillator to the atomic resonance signal (Figure 6.1):

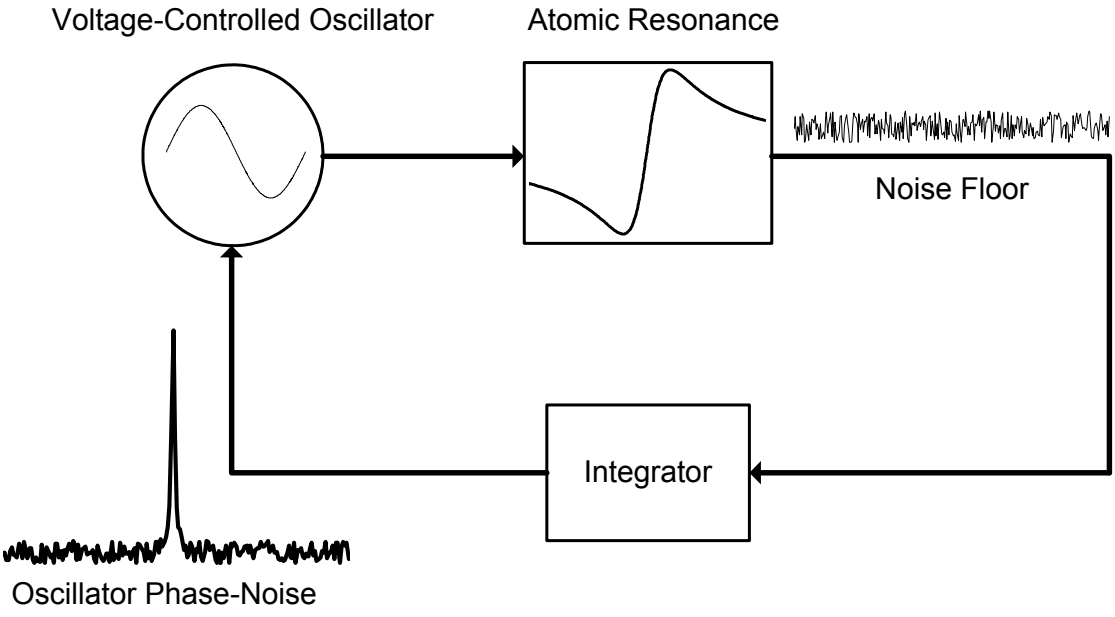


Figure 6.1: Passive Atomic Frequency Standard

Assume the slope of the voltage-controlled oscillator frequency-voltage tuning curve is $K_V$, and the slope of the atomic resonance error signal is:

$$\left(\frac{\partial E}{\partial f}\right) \tag{6.1}$$

The difference in the frequency of the voltage-controlled oscillator and the center of the atomic resonance is:

$$\Delta f = f_O - f_A \tag{6.2}$$

The transfer function of the integrator is modeled using:

$$H(s) = -\frac{1}{RCs} \tag{6.3}$$

In the figure above, the loop gain is given by the product of these three quantities:

$$A(s) = -\frac{1}{RCs} K_V \left(\frac{\partial E}{\partial f}\right) = -\frac{G}{s} \tag{6.4}$$

When the system is open loop, a noise voltage $v_n$ at the integrator input generates a signal $V_E$ proportional to $A(s)$ at the output of the atomic resonance measurement. The equation which describes the closed-loop system is:

$$(v_n + V_E)A(s) = V_E \tag{6.5}$$

and therefore

$$H_1(s) = \frac{V_E}{v_n} = \frac{A(s)}{1 - A(s)} = \frac{-G}{s + G} \tag{6.6}$$

The frequency deviation of the voltage-controlled oscillator is:

$$\Delta f = \frac{V_E}{\partial E/\partial f} \tag{6.7}$$

The transfer function between injected noise $v_n$ and the oscillator frequency deviation is:

$$\frac{\Delta f}{v_n} = \frac{1}{\left(\frac{\partial E}{\partial f}\right)} H_1(s) \tag{6.8}$$

For atomic clocks, the power spectrum of the normalized frequency deviation is conventional [1,2]:

$$y(t) \equiv \frac{f_O - f_A}{f_A} = \frac{\Delta f}{f_A} \tag{6.9}$$

The transfer function between the normalized frequency deviation and the receiver noise is:

$$\frac{y}{v_n} = \frac{1}{f_A\left(\frac{\partial E}{\partial f}\right)} H_1(s) \tag{6.10}$$

and, therefore, the power spectral density of the voltage noise $S_n$ is related to the power spectral density of the frequency deviation $S_y$ according to:

$$S_y = \frac{S_n}{{f_A}^2\left(\frac{\partial E}{\partial f}\right)^2} \left|H_1(s)\right|^2 \tag{6.11}$$

For frequency offsets within the loop bandwidth, the frequency stability is:

$$S_{y,A} = \frac{S_n}{{f_A}^2\left(\frac{\partial E}{\partial f}\right)^2} \tag{6.12}$$

The frequency stability improves by decreasing the noise floor or increasing the slope of the error signal. For example, if the slope of the error signal is 1μV / MHz, the receiver noise floor is $1nV/\sqrt{Hz}$, and the resonance frequency is 1100 MHz, then the power spectrum of the normalized frequency deviations is approximately $10^{-12}$.

To take into account the phase noise of the voltage-controlled oscillator, we can show that the overall frequency stability is [3,4]:

$$S_y = S_{y,O}\left|H_1(s)\right|^2 + S_{y,A}\left|H_2(s)\right|^2 \tag{6.13}$$

where $S_{y,O}$ is the (open-loop) frequency spectrum of the voltage-controlled oscillator, and $S_{y,A}$ is the "intrinsic" stability of the atomic resonance defined in Equation 6.12. The relationship between the power spectral density of phase and the equivalent power spectral density of the normalized frequency is [2]:

$$S_y(f) = \left(\frac{f}{f_O}\right)^2 S_\theta(f) \tag{6.14}$$

where $f$ is the offset from carrier. The function $H_1(s)$ is the low-pass characteristic defined in Equation 6.6. The "filtering" of the oscillator phase noise is a high-pass function $H_2(s)$:

$$H_2(s) = 1 - \frac{G}{s+G} = \frac{s}{s+G} \tag{6.15}$$

Therefore, well outside the loop-bandwidth, the phase-noise is the same as the open-loop noise of the oscillator; inside the loop the frequency stability is determined by the atomic resonance stability (6.12). For offset frequencies in the vicinity of the loop-bandwidth, the overall frequency noise can be calculated from (6.13).

We can also see intuitively that the feedback loop is designed to adjust the voltage at the integrator input to zero. Hence, within the loop bandwidth, noise at the integrator input is

compensated by a deviation in the voltage-controlled oscillator frequency from the center of the atomic resonance (Figure 6.2):

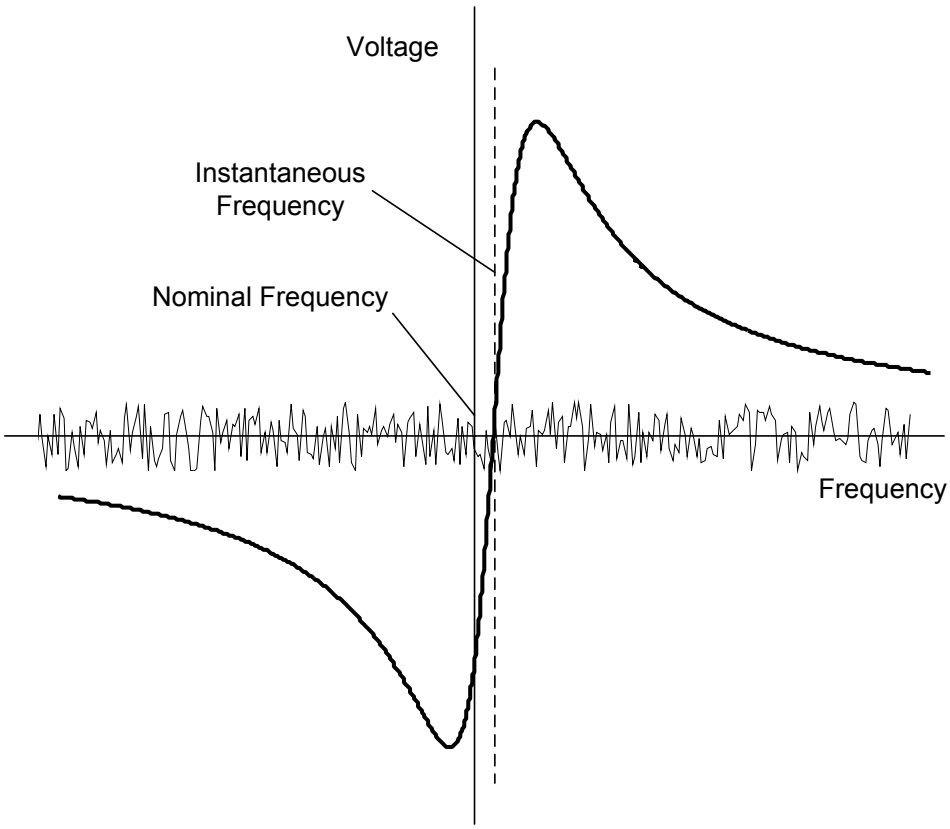


Figure 6.2: Atomic Resonance Signal showing Instantaneous and Mean Frequency

This frequency deviation is determined by the slope of the atomic resonance signal, and therefore, within the loop bandwidth:

$$\Delta f = \frac{v_n}{\left(\frac{\partial E}{\partial f}\right)} \tag{6.16}$$

This equation leads directly to (6.12). Since, as described in Equation 6.13, the best possible frequency stability inside the loop bandwidth is for a noiseless voltage-controlled

oscillator, (6.12) can be considered as the "intrinsic" stability of the atomic resonance, which is seen to depend on the measurement sensitivity and the atomic resonance width.

## 6.2 Measurement of Frequency Stability

The long-term stability of a frequency source is usually characterized in the time domain. A simple technique for measuring the frequency stability is shown below:

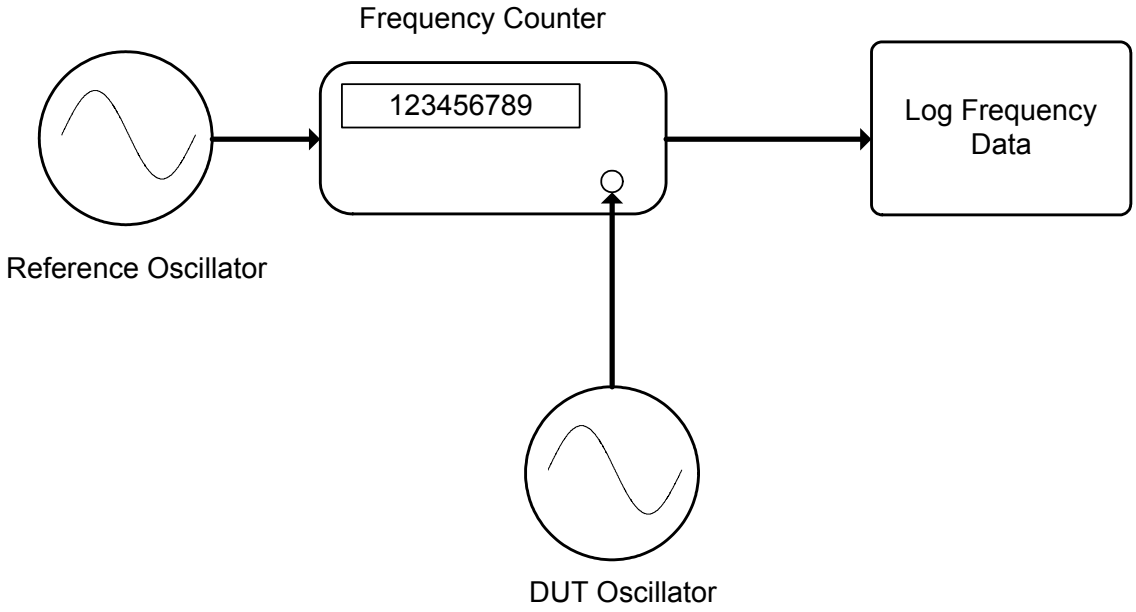


Figure 6.3 Direct Frequency Counter Measurement of Allan Variance

In Figure 6.2, a frequency counter samples the frequency of the device under test and the frequency measurement data is logged to a computer. The variations between successive frequency measurements characterize the frequency stability of the oscillator. The usual metric for the time-domain frequency stability is the two-sample variance, or Allan variance [1,2]:

$$\sigma_y{}^2(\tau) \cong \left[ \frac{1}{2(M-1)} \sum_{k=1}^{M-1} (\bar{y}_{k+1} - \bar{y}_k)^2 \right] \tag{6.17}$$

where $y$ is the normalized frequency deviation (Equation 6.9) averaged over the sampling interval:

$$y = \frac{1}{\tau} \int_{t_k}^{t_k+\tau} y(t)dt \tag{6.18}$$

The direct frequency counter technique assumes the reference oscillator internal to the frequency counter is more stable than the DUT oscillator.

The estimate of the Allan variance should also account for the dead time between measurements, as described in [5]. The article contains formulas to correct the error introduced by dead time, depending on the power-law characteristic of the noise processes. Additional measurement techniques are described in [6].

The Allan variance, defined in (6.17), and the power spectrum of the normalized frequency deviation $S_y(f)$ are related by the transformation [1]:

$$\sigma_y^2(\tau) = 2\int_0^\infty S_y(f) \frac{\sin^4(\pi f\tau)}{(\pi f\tau)^2} df \tag{6.19}$$

The transformation between the Allan variance and spectral density of the frequency fluctuations is simple when the spectral density is a power law:

$$S_y(f) = h_\alpha f^\alpha \tag{6.20}$$

White noise frequency fluctuations result in an Allan variance:

$$\sigma_y^2(\tau) = 2\int_0^\infty h_0 \frac{\sin^4(\pi f\tau)}{(\pi f\tau)^2} df = \frac{h_0}{2\tau} \tag{6.21}$$

and flicker frequency noise results in a variance [2]:

$$\sigma_y^2(\tau) = 2\int_0^\infty \frac{h_{-1}}{f}\frac{\sin^4(\pi f\tau)}{(\pi f\tau)^2}df = 2\log_e 2h_{-1} \tag{6.22}$$

White noise results in $\tau^{-1}$ scaling of the Allan variance, and 1/f noise sources result in a constant "flicker floor" in the Allan variance plot. For example, assuming the short-term stability of the passive atomic frequency standard is due to a white noise process, using (6.12) and (6.21) shows that the Allan variance is given by:

$$\sigma_{y,A}^2(\tau) = \frac{1}{2\tau}\frac{S_n}{f_A{}^2\left(\frac{\partial E}{\partial f}\right)^2} \tag{6.23}$$

The short-term stability of a frequency standard is often quoted as the Allan deviation at 1 second:

$$\sigma_{y,A}(\tau = 1) = \frac{1}{\sqrt{2}}\frac{\sqrt{S_n}}{f_A\left(\frac{\partial E}{\partial f}\right)} \tag{6.24}$$

For example, if the slope of the error signal is 1μV / MHz, the receiver noise floor is $1nV/\sqrt{Hz}$, and the resonance frequency is 1100 MHz, the Allan deviation is approximately $0.64 \times 10^{-7}$.at 1 second integration.

## 6.3 Solid-State Atomic Frequency Standard

The prototype solid-state atomic frequency standard is the same as the zero-field electron spin resonance spectrometer described in Chapter 4, with the addition of a feedback loop to lock the voltage-controlled oscillator to the center of the magnetic resonance signal (Figure 6.4):

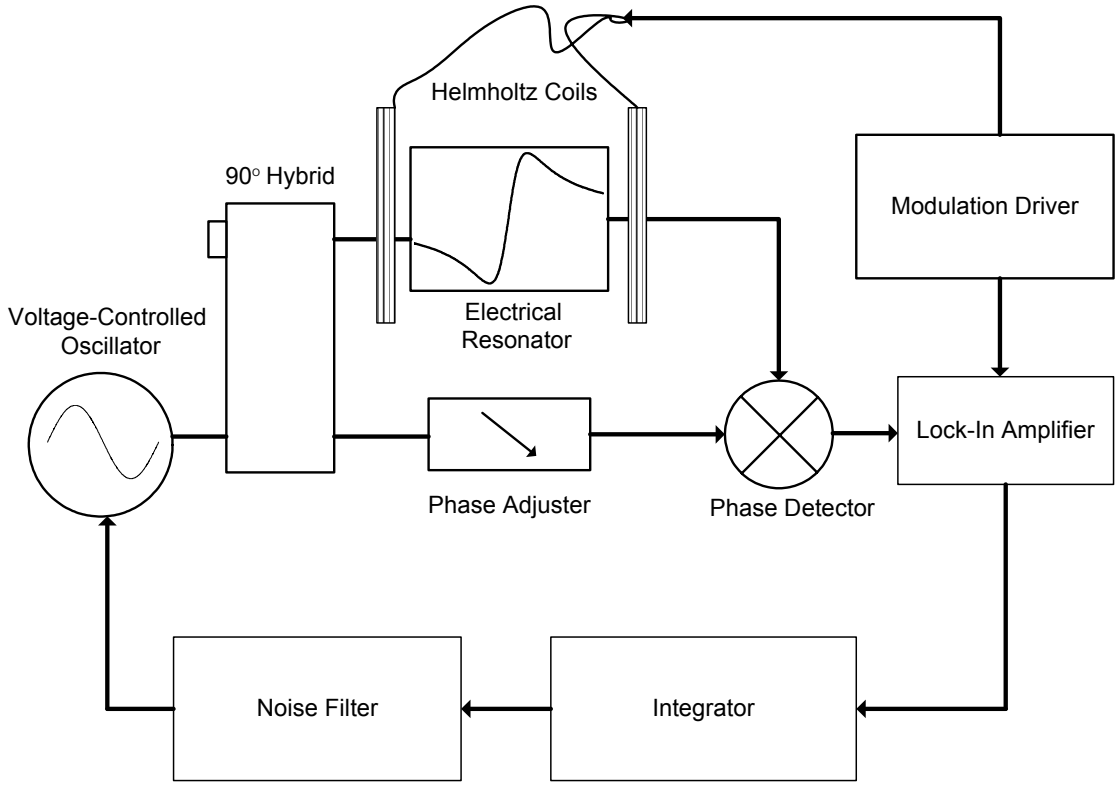


Figure 6.4 Solid-State Atomic Frequency Reference

In the prototype measurements, the bandwidth of the frequency-locking loop was approximately 1 Hz. The proof-of-concept experiment needs refinement to reduce the technical noise sources to below the fundamental random noise processes; however, frequency-locking has been demonstrated as shown on the next page in Figure 6.5:

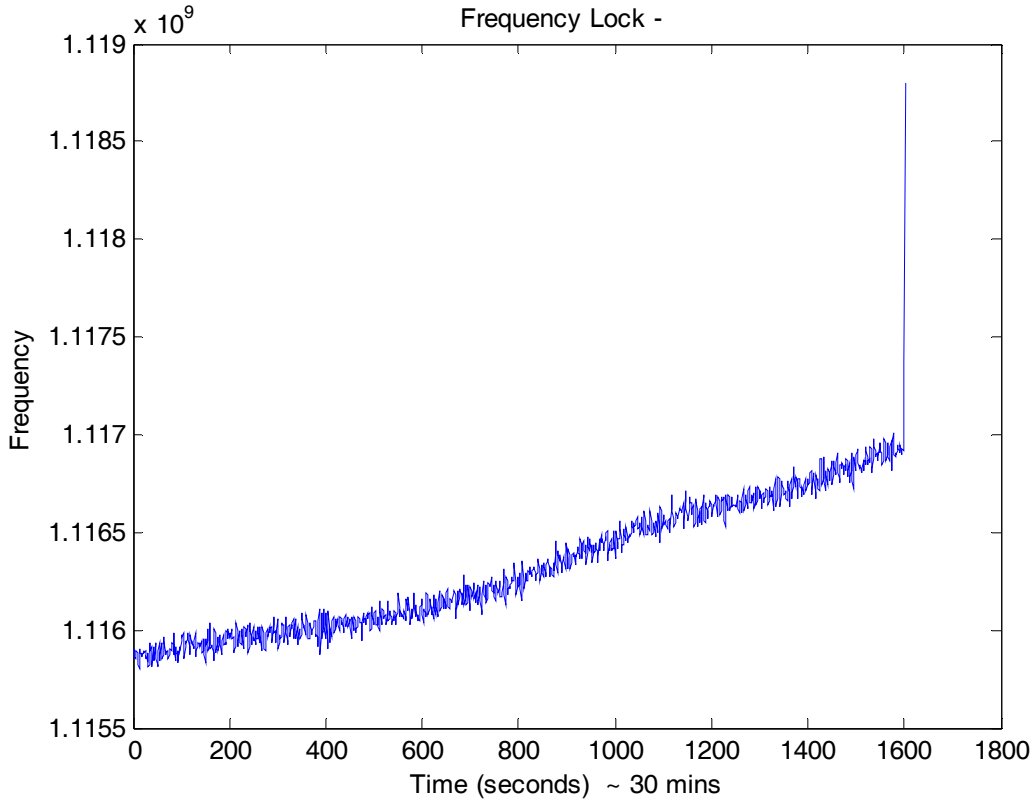


Figure 6.5 Frequency-Locking of Solid-State Atomic Frequency Standard

The solid-state atomic clock generates a reference frequency at 1116.5 MHz. The oscillator is locked to the magnetic resonance for more than 20 minutes, but shows considerable frequency drift. The frequency drift is due thermal drift of the alignment of the loop-gap resonator, which results in drift in the background interference signal from acoustic pickup. At 1600 seconds, the drift is such that the zeroing is lost and the loop comes unlocked. The short-term frequency variations are due to 60 Hz spurs close to the lock-in modulation frequency, not the random noise floor. With improvements in the design, Allan deviations at 1 second on the order of $10^{-8}$ or better appear feasible, as will be discussed in the conclusion.

## 6.4 Frequency Stability – Thermal Noise Limit

The theoretical short-term frequency stability can be calculated assuming thermal noise of the receiver is the limiting noise source. In practice, other noise sources may limit system performance; however, with proper design the magnetic resonance measurement will approach the thermal limit as discussed in Chapter 5. For example, in the prototype design, thermal drift in the alignment of the capacitive gap results in a relatively large background signal. The variations in the gap result in changes in sensitivity to the acoustics and common mode pickup. A second source of noise is spurs from 60 Hz harmonic pickup. In the current prototype these systematic noise sources mask the thermal noise floor.

The frequency stability assuming thermal noise as a limiting source is calculated using Equation 6.24. An example measurement of the vanadium magnetic resonance is shown in Figure 2.3, Chapter 2. The lock-in amplifier gain was $4 \times 10^{-6}$ and the peak-to-peak resonance signal is 1.2 μV, with a width of 6 MHz. The slope of the error signal from the atomic resonance is 0.2 μV / MHz.

The measured spectrum shown at the end of Chapter 2 (Figure 2.5) used a mixer with a 6 dB pad on the input to improve matching. The conversion gain of the mixer and attenuator loss account for 13 dB signal loss which subtracts directly from the sensitivity. If a low-noise amplifier were used ahead of the mixer, the conversion loss would not limit the sensitivity. With these assumptions, the signal may be increased by 13 dB (factor of 4.5 in voltage) to estimate the thermal limit on sensitivity. As a result, we use 0.9 μV / MHz as the error signal slope in the estimate below.

The noise of a 50 Ohm resistor at 300K is $0.9 nV / \sqrt{Hz}$. Using Equation 6.24, with a reference frequency of 1115 MHz, the thermal limit on the Allan variance at 1 second is seen to be $0.63 \times 10^{-6}$. This calculation is not a “fundamental limit” on the frequency stability, in that many additional factors, such as the concentration of paramagnetic ions, the carrier power, and the resonator design, may be optimized to improve the short-term stability.

# BIBLIOGRAPHY, CHAPTER 6

[1] IEEE Std 1139-1999, *IEEE Standard Definitions of Physical Quantities for Fundamental Frequency and Time Metrology – Random Instabilities*, March 1999.

[2] J. A. Barnes *et al.*, "Characterization of Frequency Stability," *IEEE Transactions on Instrumentation and Measurement*, vol. 20, no. 105, 1971.

[3] J. Vanier and L. Bernier, "On the Signal-to-Noise and Short-Term Stability of Passive Rubidium Frequency Standards," *IEEE Transactions on Instrumentation and Measurements*, IM-30, 277, 1981.

[4] J. Vanier, M. Tetu and L. Bernier, "Transfer of Frequency Stability from an Atomic Reference to a Quartz-Crystal Oscillator," *IEEE Transactions on Instrumentation and Measurements*, (1979), IM-28, 188

[5] J. A. Barnes and D. W. Allan, "Variances Based on Data with Dead Time between the Measurements," *NIST Technical Note 1318*, 1990.

[6] J. Vanier and M. Tetu, "Time Domain Measurement of Frequency Stability" *Proc. 10th PTTI Meeting*, pp. 247-291, Nov. 1978.

*Chapter 7*

# CONCLUSION

The dissertation has developed the original concept of a solid-state atomic clock, and presented, in detail, a prototype system to realize the concept. The prototype system uses only low-cost radio-frequency components which may easily be integrated into a compact atomic frequency standard. The "atomic" resonance signal was derived from the zero-field electron spin resonance of divalent vanadium in a magnesium oxide lattice. The thesis also showed an original measurement of the zero-field magnetic resonance of vanadium in magnesium oxide.

As was discussed in Chapter 3, for the $m_F = 0$ to $m_F = 0$ magnetic field independent transitions, there is an optimal concentration of paramagnetic ions which increases the paramagnetic resonance signal without significantly increasing the resonance width. The maximum concentration is limited by exchange coupling or second-order dipolar broadening. For magnetic resonance lines with a first-order Zeeman shift, the short-term stability is independent of concentration, because the dipolar resonance width increases in proportional to concentration. With increased doping, the slope of the magnetic resonance signal is unchanged, and therefore the frequency stability is constant (Chapter 6, Equation 6.24). This is why the existence of a second-order magnetic field independent transition is so significant for the performance of a small solid-state atomic clock, because it implies the possibility of increasing the signal intensity without first-order broadening of the resonance width.

A second topic for further study is the effect of higher order terms proportional to $\mathbf{S}^3$ on the apparent resonance width at zero-field, considered at the beginning of Chapter 2. These additional terms in the vanadium spin Hamiltonian may account for the asymmetry of the resonance signal measured in Figure 2.3.

The temperature dependence of the zero-field magnetic resonance was not investigated in this thesis. However, previous high-field measurements (Chapter 2, [12]) indicate the temperature coefficient of divalent vanadium in magnesium oxide is on the order of a few parts-per-million per degree. The hyperfine resonance frequency would decrease with increasing temperature. However, very careful measurements on the higher order terms in the isoelectronic $Cr^{3+}$/MgO system showed that the factors proportional to $\mathbf{S}^3$ have strong positive temperature dependence (Chapter 2, [16]). Hence, the combined effect of the hyperfine splitting and the higher order terms may reduce the overall temperature dependence at zero-field. Another possibility is to look at different materials systems where the Hamiltonian is a combination of hyperfine and crystal field terms, or to look at multiple dopants in a signal crystal, to minimize the measured temperature coefficient.

Therefore, several research questions remain, as far as the possibilities for exploiting narrow magnetic field independent transitions to optimize the short-term stability, and the possibilities of developing a materials system with reduced temperature dependence or even a turn-over temperature. The best technique for measuring the magnetic field independent transitions is also an open question, where we have suggested the possibility of a "rotating polarization" measurement as one solution.

The short-term stability is always a trade-off with the volume of the resonator, because for a larger resonator, the RF magnetic field density is lower at a given carrier power, and generally, the unloaded quality factor Q of the resonator increases. For example, the Q of a loop-gap resonator is approximately 500. This trade-off with sample volume is similarly the case for miniaturized rubidium atomic clocks.

There is no "one answer" for the frequency stability of the solid-state atomic frequency standard – the theoretical stability will depend largely on the acceptable power consumption. In particular, for a large resonator volume, the power to drive the audio magnetic field is considerable. Similarly, regulating the temperature of a large resonator uses considerable power. The trade-offs involving power consumption and the volume (*i.e.*, unloaded-Q) of the resonator are characteristic of oscillator design in general, provided

thermal noise is dominant and not excess device noise, or other noise sources which scale with carrier power.

Several improvements in the prototype design were also suggested in Chapters 4, 5, and 6, which are summarized below:

- adding carrier suppression or using a second frequency discriminator to demonstrate a thermal noise limited measurement at high carrier power
- miniaturization of the electrical resonator, and reduction in sensitivity to acoustics
- ceramic manufacturing of high purity vanadium doped magnesium oxide and developing an optimal heat treatment recipe
- finding the optimal doping concentration for best short-term stability by analysis of the second-order dipolar broadening of the magnetic field independent transitions
- studies of the long-term stability of solid-state atomic frequency standard

The goal is to demonstrate a spectrometer with noise performance limited by the receiver noise figure. In the current demonstration, technical noise sources remain the limiting factors. We anticipate a significant improvement in the measured short-term stability with the use of narrow magnetic-field independent resonances and better spectrometer sensitivity.

In conclusion, this work opens the possibility for developing a commodity frequency standard with short-term stability and accuracy in the range of $10^{-7}$ to $10^{-9}$. The new frequency standard is entirely solid-state, works at room temperature, and without large magnetic fields or hermetic packaging. The possibilities for long-term stability better than crystal oscillators make the solid-state atomic frequency standard an interesting technology to address the needs of a number of communications and navigation systems, for both military and next-generation consumer products.